

Experimental investigation on fractal drilling strength

Alberto Carpinteri, Luciano Dimastrogiovanni and Nicola Pugno *

Department of Structural Engineering, Politecnico di Torino, Corso Duca degli Abruzzi 24, 10129 Torino, Italy

Received 31 May 2004

Abstract. In this paper we present an experimental investigation on fractal drilling strength, theoretically introduced on the basis of the universal fragmentation laws. We focus our attention on impregnated hard grain bit drilling with different base materials, tools and types of control, during steady state or transient condition perforations. Some single scratch tests with abrasive grains or hard material cutting edges, complete the analysis. A very strong size-effect on classical drilling strength emerges. On the other hand, the fractal drilling strength can be considered as a size-independent property. A comparison between classical and fractal approaches is thus presented.

1. Introduction

Drilling perforations are extensively used in engineering applications at different size- and time-scales, i.e., by varying the size of the material removed, as well as the drilling velocity. To describe drilling resistance for a given material, the so-called drilling strength S is typically introduced: it is defined as the ratio between the power consumption and the volume removed per unit time and it is usually assumed as a material constant [1].

On the other hand, only recently, the Authors [2], on the basis of universal fragmentation laws [3], have shown how the drilling fragmentation should be considered as a fractal or multi-scale phenomenon. The main consequence of this approach is the prediction of strong size- and time-effects on nominal drilling strength and the introduction of the so-called fractal drilling strength Γ , a size- and time-independent parameter, with anomalous physical dimensions [2].

Several theoretical models have been proposed linking fractals [4,5] to fracture and fragmentation [6,7]. Carpinteri and Pugno have recently presented an application of fractals to fracture and fragmentation in different scientific areas [8]. Carpinteri [9] and Carpinteri et al. [10–12] used the fractal and multifractal approaches to explain the scaling laws for strength and toughness in the breaking behaviour of disordered materials. Engleman et al. [13] applied the maximum entropy method to show that the number-size distribution follows a fractal law for fragments that are not too large. By combining a fractal analysis of brittle fracture with an energy balance, a theoretical expression for the fragment size distribution is derived as a function of energy density [14,15]. In [16] the fragment size distribution is predicted from clusters of connected bonds in a cubic lattice and using percolation theory. A suite of

*Corresponding author. Tel.: +39 115644902; Fax: +39 115644899; E-mail: pugno@polito.it.

fractal models has been developed in [17–22]; these Authors use the probabilities of failure to predict the fragment-size distribution based on the geometrical properties of the original material. A review on drilling indentation and the physical mechanisms of hard rock fragmentation under mechanical loading has been performed in [23]; an experimental analysis of the variation of drilling detritus with operating parameters has been reported in [24].

In the present paper, we describe an experimental investigation on the mentioned fractal drilling strength, which was theoretically introduced in [2] on the basis of the universal fragmentation laws [3]. A multifractal extension has been also proposed by the same Authors [25]. We focus our attention on different base materials (limestone, sandstone, quartz and concrete), different impregnated hard grain bit tools (by varying their grains' content and size), different test controls (power consumption and drilling velocity) in steady state or transient conditions. Some tests on cutting, performed by single scratch hard grain or hard metal cutting edge, complete the analysis. As predicted by the fractal approach, very strong size and time-effects on classical drilling strength emerge.

2. Nominal or multi-scale drilling strengths

From the experiments, the nominal drilling strength S can be estimated as the ratio of the power dissipated in the comminution process to the volume removed per unit time [1,2]:

$$S \cong \frac{\eta \dot{W}}{(1 + \varepsilon) A \dot{\delta}}, \quad (1)$$

where \dot{W} is the power of the engine, $\eta \approx 0.9$ is its efficiency, $(1 + \varepsilon)A \approx 1.1A$ is the effective area of the tool ring (larger by about 10% than the cross section area A of the tool) and $\dot{\delta}$ is the drilling velocity.

On the other hand, the fractal drilling strength Γ can be evaluated by definition as the ratio of the power dissipated to the measure of a domain intermediate between surface and volume [2], as follows:

$$\Gamma \cong \frac{\eta \dot{W}}{((1 + \varepsilon) A \dot{\delta})^\gamma}. \quad (2)$$

In this hypothesis, between the two quantities there is the following correlation:

$$S \cong \frac{\Gamma}{(A \dot{\delta})^\gamma}. \quad (3)$$

The fractal drilling strength presents the anomalous dynamic units of $\text{N m}^{1-3\gamma} \text{s}^{\gamma-1}$. The fractal drilling strength is a constant, which is independent of the drilling velocity and of the area of the tool. On the other hand, we expect the nominal drilling strength S to be dependent on drilling velocity and tool area, according to Eq. (3). For drilling, the energy dissipation is supposed to occur on a surface, as experimentally verified [2], so that $\gamma = 2/3$, on the other hand, classically $\gamma = 1$ and fractal and drilling strengths coincide.

3. Single scratch tests – influence of size scale

In the single scratch tests, A coincides with the transversal cross-section area of the scratch and δ with the linear cutting velocity.

Experimentally, it is very evident that the nominal drilling strength is drilling velocity and tool area dependent, as described in Figs 1 and 2 for limestone. It decreases with an increase in size A and/or in drilling velocity δ , as predicted by Eq. (3). The nominal drilling strength S from the scratch test (small scale) is approximately equal to 35 GPa, i.e. larger at least by one order of magnitude than the value obtained from the drilling tests (1 GPa), which is again by one order of magnitude larger than the value obtained for very large scales (0.03 GPa), coinciding with the compressive strength σ_C of the material [1,2]. As expected, the drilling strength strongly increases by decreasing the size.

The same results have been confirmed by single scratch tests at small scale on concrete ($S \approx 20$ GPa), sandstone ($S \approx 3$ GPa) and quartz ($S \approx 20$ GPa).

As predicted by the fractal approach – Eq. (3), $\gamma = 2/3$ – the slope in the bi-logarithmic diagram drilling strength versus size scale (cubic root of the removed volume) is around -1 (Fig. 3). The first four data on the left in Fig. 3 are related to single scratch hard grain tests. The experiment on the largest size has been performed by a hard metal cutting edge tool. A linear best-fit approximation for the single scratch hard grain tests shows a slope of -1.21 ($R^2 = 0.97$). This means that the fractal drilling strength can be considered as size-independent. It is important to emphasize that the classical assumption $S \approx \sigma_C$ [1] can be used only at very large scales. On the contrary, at very small scales S becomes larger by approximately three orders of magnitude.

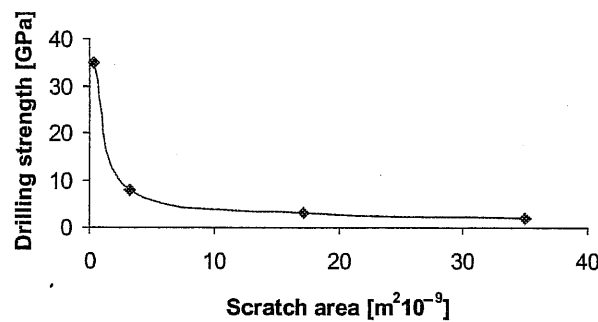


Fig. 1. Drilling strength vs scratch area (limestone).

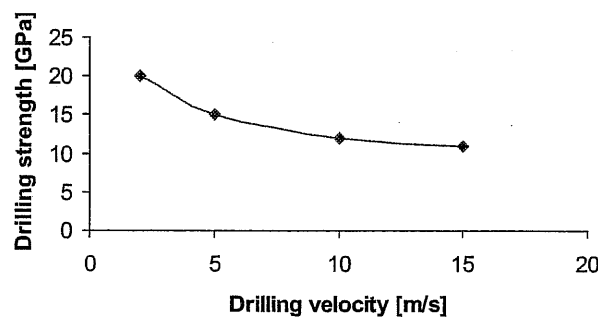


Fig. 2. Drilling strength vs drilling velocity (limestone).

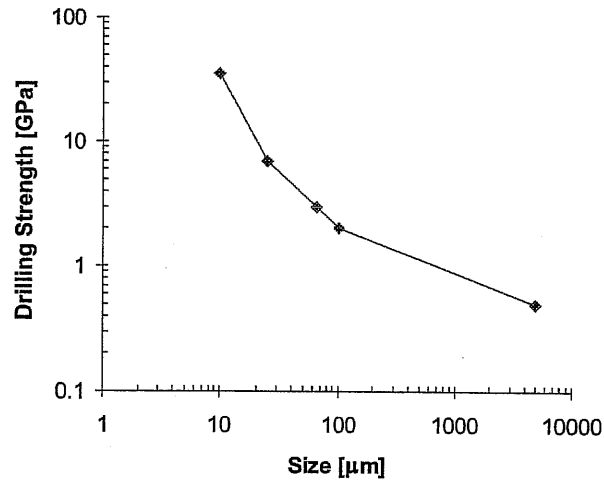


Fig. 3. Single scratch tests: size effect on cutting (or drilling) strength (limestone).

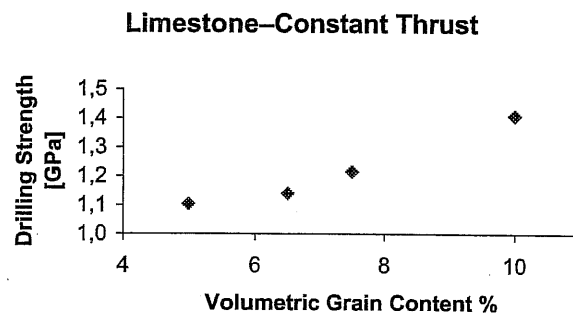


Fig. 4. Drilling strength as a function of the hard grain content in force-controlled tests (limestone).

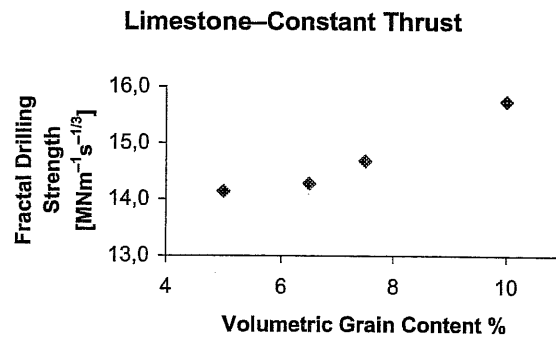


Fig. 5. Fractal drilling strength as a function of the hard grain content in force-controlled tests (limestone).

4. Drilling tests on limestone – influence of tool hard grain content

Some drilling experiments to evaluate the influence of the tool volumetric hard grain content on the nominal and fractal drilling strengths, have been carried out. The radius and thickness of the tool are respectively $R = 51 \text{ mm}$ and $t = 3.5 \text{ mm}$ ($A = 2\pi Rt$).

The drilling strength S can be estimated by means of Eq. (1); experimentally, it appears to be of the order of magnitude of 1 GPa (see Figs 4 and 6). On the other hand, the fractal drilling strength Γ can be evaluated by means of Eq. (2) and experimentally it appears to be of the order of magnitude of $15 \text{ MN m}^{-1} \text{ s}^{-1/3}$ (see Figs 5 and 7).

The average experimental results from force-controlled tests are summarized in Table 1. The nominal and fractal drilling strengths are presented in Figs 4 and 5 as functions of the hard grain content. A rea-

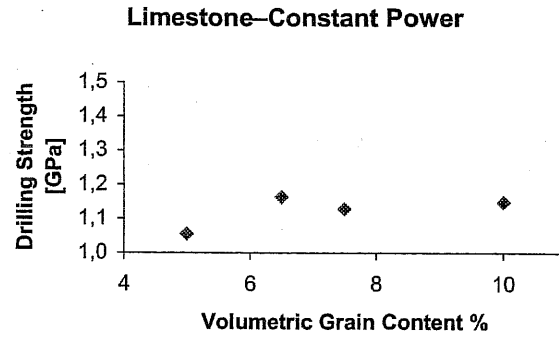


Fig. 6. Drilling strength as a function of the hard grain content in power-controlled tests (limestone).

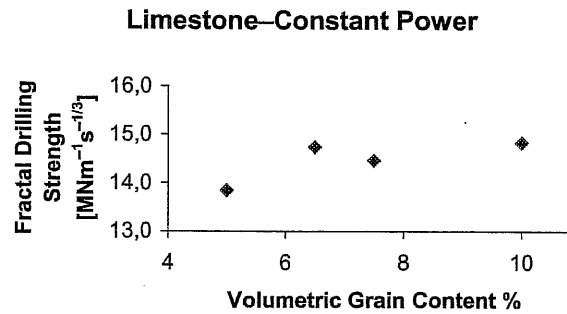


Fig. 7. Fractal drilling strength as a function of the hard grain content in power-controlled tests (limestone).

Table 1

Average results from force-controlled tests on limestone [SI]

Volumetric hard grain content %	Thrust force $F = \text{constant}$	Drilling velocity $\dot{\delta}$	Power consumption \dot{W}	Rotation speed $\dot{\varphi}$
5.0	1370	0.00171	2584	45.84
6.5	1370	0.00159	2485	46.05
7.5	1370	0.00143	2381	47.62
10.0	1370	0.00113	2182	49.93

sonable increase with hard grain content is shown. As a matter of fact, if the hard grain content increases the force on a single grain (at constant thrust) as well as its penetration decrease, so that the drilling strength increases (Fig. 3).

The average experimental results from power-controlled tests are summarized in Table 2. The nominal and fractal drilling strengths are presented in Figs 6 and 7 as functions of the hard grain content. They appear substantially constant.

5. Drilling tests on concrete – influence of tool hard grain content

Some drilling experiments to evaluate the influence of the volumetric hard grain content on nominal and fractal drilling strengths have been performed. The drilling tests on concrete are force- or power-controlled. The radius and thickness of the tool are the same as already considered.

The average experimental results for force-controlled tests are summarized in Table 3. The same trends are observed also for the power-controlled tests, in which also the thrust appears approximately constant.

Table 2

Average results from power-controlled tests on limestone [SI]

Volumetric hard grain content %	Thrust force F	Drilling velocity $\dot{\delta}$	Power consumption $\dot{W} \cong \text{constant}$	Rotation speed $\dot{\varphi}$
5.0	1371	0.00183	2646	43.65
6.5	1477	0.00165	2630	42.39
7.5	1567	0.00171	2643	43.54
10.0	1824	0.00175	2752	42.39

Table 3

Average results from force-controlled tests on concrete [SI]

Volumetric hard grain content %	Thrust force $F = \text{constant}$	Drilling velocity $\dot{\delta}$	Power consumption \dot{W}	Rotation speed $\dot{\varphi}$
5.0	1426	0.00098	1788	52.63
6.5	1426	0.00090	1701	53.01
7.5	1426	0.00096	1776	53.20
10.0	1426	0.00078	1596	53.90

Concrete-Constant Thrust

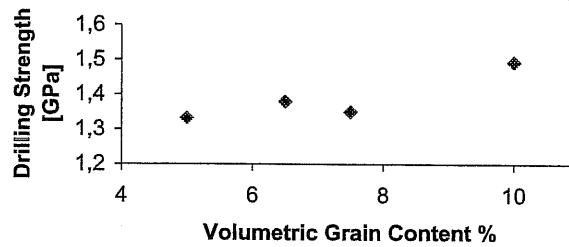


Fig. 8. Drilling strength as a function of the hard grain content in force-controlled tests (concrete).

Concrete-Constant Thrust

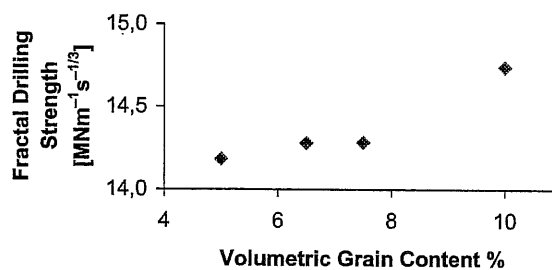


Fig. 9. Fractal drilling strength as a function of the hard grain content in force-controlled tests (concrete).

The drilling strength S can be estimated by means of Eq. (1); experimentally, it appears to be of the order of magnitude of 1 GPa (see Fig. 8), as theoretically predicted by the analysis of drilling detritus [2]. On the other hand, the fractal drilling strength Γ can be evaluated by means of Eq. (2) and experimentally it appears to be of the order of magnitude of $14 \text{ MN m}^{-1} \text{ s}^{-1/3}$ (see Fig. 9).

6. Influence of hard grain size and drilling depth

Some experiments on transient drilling perforation have been carried out. We have used a new tool with sharp hard grains of different sizes. During the life of the tool, or along with the drilling depth, the hard grains change their cutting ability. After a transient regime, the process reaches a steady state condition, as previously treated in Sections 4 and 5. On the other hand, in the present section and in Section 7, we focus our attention on the mentioned transient process.

The experiments emphasize how the main parameter influencing the drilling response is the power consumption. The experimental curves and the theoretical predictions according to Eqs (1) and (2) and assuming the nominal or the fractal drilling strengths as constants, are reported respectively in Figs 10a

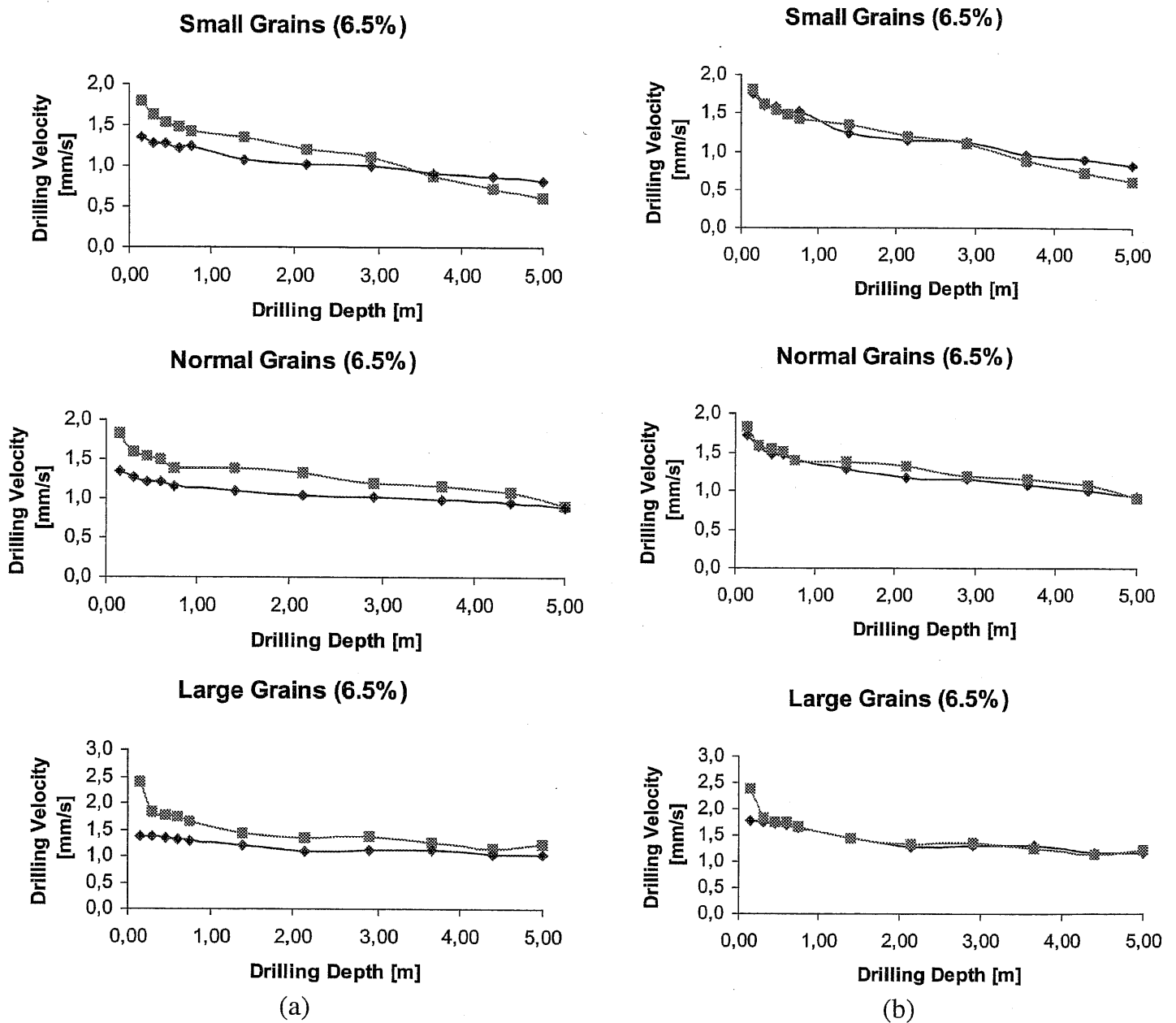


Fig. 10. (a) Experimental results (squares) and theoretical predictions (rhombs) from Eq. (1). (b) Experimental results (squares) and theoretical predictions (rhombs) from Eq. (2).

and 10b, for concrete ($S = 1.4$ GPa or $\Gamma = 14$ MN m⁻¹ s^{-1/3}) and with a hard grain content of 6.5%. Similar results have been obtained for hard grain contents of 5, 7.5 and 10%, on concrete and limestone.

In Figs 10a and 10b, the comparison between experimental results and, respectively, nominal and fractal theoretical predictions are presented, by varying the hard grain size. Three different hard grain sizes are considered: ≈ 100 (small), ≈ 300 (normal) and ≈ 500 (large) micrometers.

A significant discrepancy is shown only for the nominal evaluation, whereas fractal theoretical predictions and experimental results agree very satisfactorily.

7. Pseudo-friction coefficient

The hard grain cutting ability changes with the hard grain volumetric content, dimension and quality (sharp, blunt, and broken hard grains), during the drilling process. To model these effects from a global point of view, a pseudo-friction coefficient μ can be defined:

$$\mu = \frac{M_t}{FR}, \quad (4)$$

where M_t is the torque, F the thrust force and R the radius of the tool.

The influence of the hard grain content on the pseudo-friction coefficient (evaluated as $\mu = (\eta\dot{W})/(FR\dot{\phi})$) is reported in the experimental Figs 11a,b and 12.

The influences of the hard grain size and of the drilling depth on the pseudo-friction coefficient are shown in Fig. 13. It is very interesting to note that the pseudo-friction coefficient decreases with a hard grain content increase and/or with a hard grain dimension decrease, as well as with the life of the tool

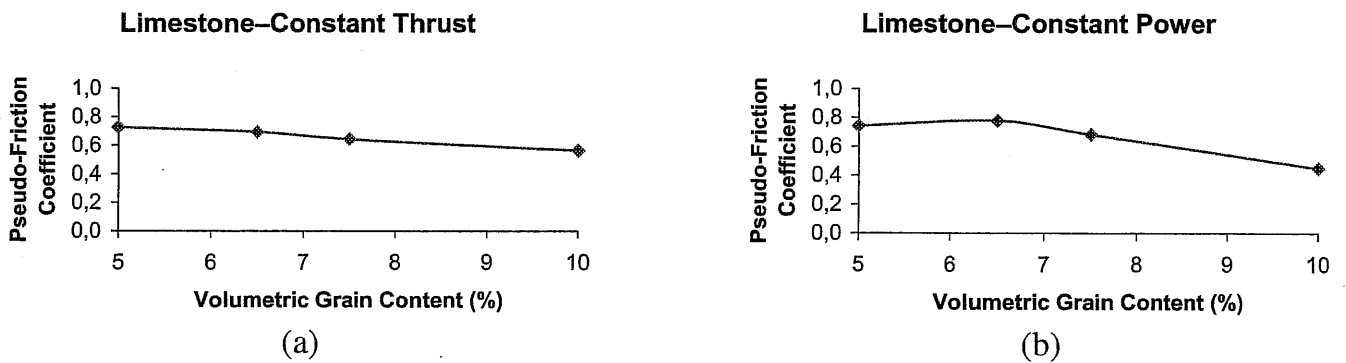


Fig. 11. (a) Pseudo-friction coefficient vs hard grain content (constant thrust-limestone). (b) Pseudo-friction coefficient vs hard grain content (constant power-limestone).

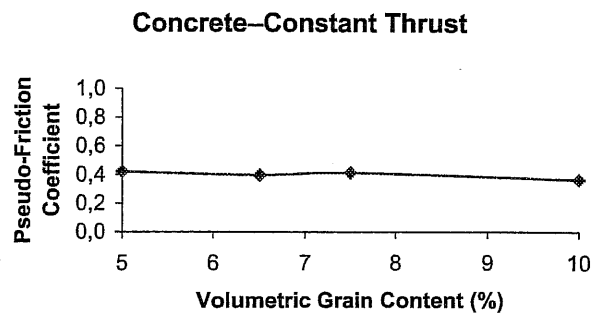


Fig. 12. Pseudo-friction coefficient vs hard grain content (constant thrust-concrete).

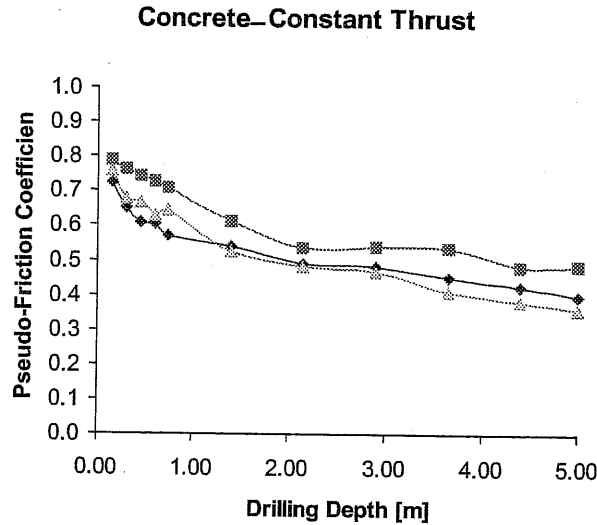


Fig. 13. Pseudo-friction coefficient vs drilling perforation. Comparison between large (squares), normal (rhombuses) and small hard grains (triangles). Hard grain content = 6.5%.

Table 4a

Pseudo-friction coefficients in concrete for new and steady state condition tools. Influence of hard grain dimension

Small hard grain		Normal hard grain		Large hard grain	
New tool	Used tool	New tool	Used tool	New tool	Used tool
0.75	0.35	0.75	0.40	0.80	0.50

Table 4b

Pseudo-friction coefficients in concrete and limestone. Influence of hard grain content

	μ	
	5%	10%
Concrete	0.4	0.4
Limestone	0.70	0.50

(or the drilling depth). It tends to become a constant for steady state processes. The main results are summarized in Tables 4a and 4b.

By means of the pseudo-friction coefficient, we are able to predict the drilling velocity also for transient force-controlled processes. From Tables 4a and 4b we can obtain the pseudo-friction coefficient for the considered case (for a steady state process, μ is time- and drilling depth-independent), from Eq. (4) the torque, from the engine characteristics (connecting torque and rotational speed) the rotational speed and, finally, from Eq. (3), the drilling velocity.

8. Conclusions

We have presented an experimental investigation on the nominal and fractal drilling strengths. It has been shown how the nominal drilling strength S at small scales, obtained from scratch tests, is experimentally larger by at least one order of magnitude than the value obtained from the usual drilling tests, which is again by one order of magnitude larger than the value obtained for very large scales, coinciding

with the compressive strength of the material [1]. The size effects on nominal drilling strength are shown in Fig. 3. This means that the nominal drilling strength can not be considered, as usually assumed, size-independent. On the other hand, the slope of the size effect in the bi-logarithmic diagram of Fig. 3 is close to -1 , as predicted by the fractal approach. As a consequence, the fractal drilling strength can be considered as size-independent. According to this consideration, the experimental comparisons of nominal and fractal evaluation show a significant discrepancy only for the former, whereas fractal theoretical predictions and experimental results agree very satisfactorily.

References

- [1] J. Paone and W.E. Bruce, *Drillability Studies – Diamond Drilling*, USBM-RI 6324, 1963.
- [2] A. Carpinteri and N. Pugno, A fractal comminution approach to evaluate the drilling energy dissipation, *Int. J. of Numerical and Analytical Methods in Geomechanics* **26** (2002), 499–513.
- [3] A. Carpinteri and N. Pugno, One-, two- and three-dimensional universal laws for fragmentation due to impact and explosion, *Journal of Applied Mechanics* **69** (2002), 854–856.
- [4] B.B. Mandelbrot, *The Fractal Geometry of Nature*, Freeman, New York, 1982.
- [5] J. Feder, *Fractals*, Plenum Publishing Corporation, New York, 1988.
- [6] D. Béla Beke, *Principles of Comminution*, Publishing House of the Hungarian Academic of Sciences, 1964, pp. 90–92.
- [7] D.L. Turcotte, *Fractals and Chaos in Geology and Geophysics*, Cambridge University Press, 1992, pp. 20–32.
- [8] A. Carpinteri and N. Pugno, Multi-scale energy dissipation during impact and explosion fragmentation of quasi-brittle materials, in: *Int. Conf. on New Challenges in Mesomechanics*, August 26–30, 2002, Aalborg University, Denmark.
- [9] A. Carpinteri, Scaling laws and renormalization groups for strength and toughness of disordered materials, *Int. J. Solids and Structures* **31** (1994), 291–302.
- [10] A. Carpinteri and B. Chiaia, Multifractal scaling laws in the breaking behaviour of disordered materials, *Chaos, Solitons and Fractals* **8** (1997), 135–150.
- [11] A. Carpinteri, G. Ferro and I. Monetto, Scale effects in uniaxially compressed concrete specimens, *Magazine of Concrete Research* **51** (1999), 217–225.
- [12] A. Carpinteri and N. Pugno, Friction and specimen slenderness influences on dissipated energy density of quasi-brittle materials in compression: an explanation based on fractal fragmentation theory, in: *Int. Con. Fracture Mechanics of Concrete Structures-4*, May 28–June 2, 2001, Cachan, France, pp. 665–668.
- [13] R. Engleman, N. Rivier and Z. Jaeger, Size distribution in sudden breakage by the use of entropy maximization, *J. Appl. Phys.* **63** (1988), 4766–4768.
- [14] H. Nagahama, Fractal fragment size distribution for brittle rocks, *Int. J. Rock Miner. Sci. Geomech. Abstr.* **30** (1993), 469–471.
- [15] Z. Yong and M.T. Hanson, A rotational source of plane fractals and its application to fragmentation analysis of thin plates, *Chaos, Solitons and Fractals* **7** (1996), 31–40.
- [16] A. Aharony, A. Levi, R. Englman and Z. Jaeger, Percolation model calculations of fragment properties, *Ann. Israel Phys. Soc.* **8** (1986), 112–119.
- [17] E. Perfect, Fractal models for the fragmentation of rocks and soils: a review, *Engineering Geology* **48** (1997), 185–198.
- [18] M. Matsushita, Fractal viewpoint of fracture and accretion, *J. Phys. Soc. Jap.* **54** (1985), 857–860.
- [19] D.L. Turcotte, Fractal and fragmentation, *J. Geophys. Res.* **91** (1986), 1921–1926.
- [20] D.L. Turcotte, Fractals in geology and geophysics, *Pure Appl. Geoph.* **131** (1989), 171–196.
- [21] M. Rieu and G. Sposito, Fractal fragmentation, soil porosity and soil water properties: I. Theory, *Soil Sci. Soc. Am. J.* **55** (1991), 1231–1238.
- [22] J.W. Crawford, B.D. Sleeman and J.M. Young, On the relation between number size distributions and the fractal dimension of aggregates, *J. Soil Sci.* **44** (1993), 555–565.
- [23] L.L. Mishnaevsky, Physical mechanisms of hard rock fragmentation under mechanical loading: a review, *Int. J. Rock Mech. Min. Sci. & Geomech. Abstr.* **32** (1995), 763–766.
- [24] A. Ersoy and M.D. Waller, Drilling detritus and the operating parameters of thermally stable PDC core bits, *Int. J. Rock Mech. Sci.* **34** (1997), 1109–1123.
- [25] A. Carpinteri and N. Pugno, A multifractal comminution approach for drilling scaling laws, *Powder Technology* **131** (2003), 93–98.